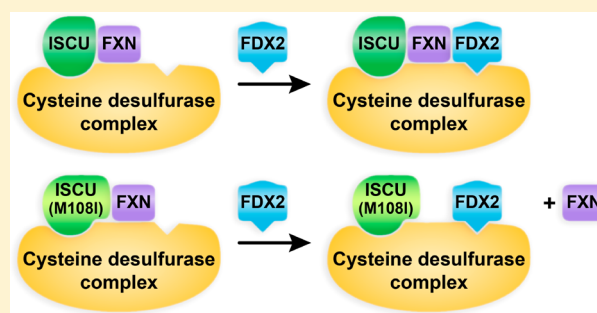


ISCU(M108I) and ISCU(D39V) Differ from Wild-Type ISCU in Their Failure To Form Cysteine Desulfurase Complexes Containing Both Frataxin and Ferredoxin

Kai Cai, Ronnie O. Frederick, Marco Tonelli, and John L. Markley*^{1b}

National Magnetic Resonance Facility at Madison and Department of Biochemistry, University of Wisconsin—Madison, 433 Babcock Drive, Madison, Wisconsin 53706, United States

ABSTRACT: Whereas iron–sulfur (Fe–S) cluster assembly on the wild-type scaffold protein ISCU, as catalyzed by the human cysteine desulfurase complex (NIA)₂, exhibits a requirement for frataxin (FXN), in yeast, ISCU variant M108I has been shown to bypass the FXN requirement. Wild-type ISCU populates two interconverting conformational states: one structured and one dynamically disordered. We show here that variants ISCU(M108I) and ISCU(D39V) of human ISCU populate only the structured state. We have compared the properties of ISCU, ISCU(M108I), and ISCU(D39V), with and without FXN, in both the cysteine desulfurase step of Fe–S cluster assembly and the overall Fe–S cluster assembly reaction catalyzed by (NIA)₂. In the cysteine desulfurase step with dithiothreitol (DTT) as the reductant, FXN was found to stimulate cysteine desulfurase activity with both the wild-type and structured variants, although the effect was less prominent with ISCU(D39V) than with the wild-type or ISCU(M108I). In overall Fe–S cluster assembly, frataxin was found to stimulate cluster assembly with both the wild-type and structured variants when the reductant was DTT; however, with the physiological reductant, reduced ferredoxin 2 (rdFDX2), FXN stimulated the reaction with wild-type ISCU but not with either ISCU(M108I) or ISCU(D39V). Nuclear magnetic resonance titration experiments revealed that wild-type ISCU, FXN, and rdFDX2 all bind to (NIA)₂. However, when ISCU was replaced by the fully structured variant ISCU(M108I), the addition of rdFDX2 to the [NIA–ISCU(M108I)–FXN]₂ complex led to the release of FXN. Thus, the displacement of FXN by rdFDX2 explains the failure of FXN to stimulate Fe–S cluster assembly on ISCU(M108I).



Iron–sulfur (Fe–S) clusters are ancient protein prosthetic groups that are involved in numerous biological processes.^{1–3} Biogenesis of Fe–S clusters is conserved in all kingdoms of life.^{4–6} The Fe–S cluster biosynthesis (ISC) machinery in human mitochondria, which involves at least 18 proteins, can be divided into two major steps: cluster assembly on the scaffold protein and cluster transfer to recipient proteins.^{7–9} Defects in protein components of the human mitochondrial ISC machinery have been associated with numerous diseases.^{10,11}

Central to the ISC machinery is the pyridoxal 5′-phosphate (PLP)-dependent protein cysteine desulfurase, which catalyzes the conversion of cysteine to alanine and mobilizes the released sulfur for cluster assembly.^{12,13} Unlike its bacterial homologue (IscS), human cysteine desulfurase (NFS1) requires two small accessory proteins, namely, ISD11 and acyl carrier protein (ACP), for full function and stability. ISD11, also known as LYRM4, is a member of the LYRM (Leu-Tyr-Arg motif) protein family.^{14,15} ACP is well-known to function in mitochondrial fatty acid biosynthesis through reactions involving its 4′-phosphopantethiene (4′-PPT) cofactor, which is conjugated to a conserved serine residue.^{16,17} Recently, yeast Acp1 was also found to be an essential component of the

cysteine desulfurase complex.¹⁸ We demonstrated that *Escherichia coli* Acp substitutes for human mitochondrial ACP in the cysteine desulfurase complex produced by co-expressing human ISD11 and NFS1 in *E. coli* cells and determined the stoichiometry to be [NFS1]₂:[ISD11]₂:[Acp]₂,¹⁹ henceforth abbreviated as (NIA)₂. This stoichiometry has been confirmed by two recently published X-ray structures of (NIA)₂ complexes prepared by overexpressing NFS1 and ISD11 in *E. coli* cells, although, curiously, the two structures exhibit quite different quaternary architecture.^{20,21}

In the *E. coli* system, IscX-Fe²⁺ has been shown to serve as the iron donor for *in vitro* Fe–S cluster assembly on IscU catalyzed by IscS.²² However, IscX has no eukaryotic homologue, and the identity of the iron donor in mitochondrial Fe–S cluster biosynthesis has remained controversial. Frataxin (FXN), a protein whose defects are associated with the common neurodegenerative disease, Friedreich ataxia,²³ has been proposed as the iron donor because of its ability to bind iron and donate iron for *in vitro* Fe–S cluster assembly

Received: December 8, 2017

Revised: February 6, 2018

Published: February 6, 2018

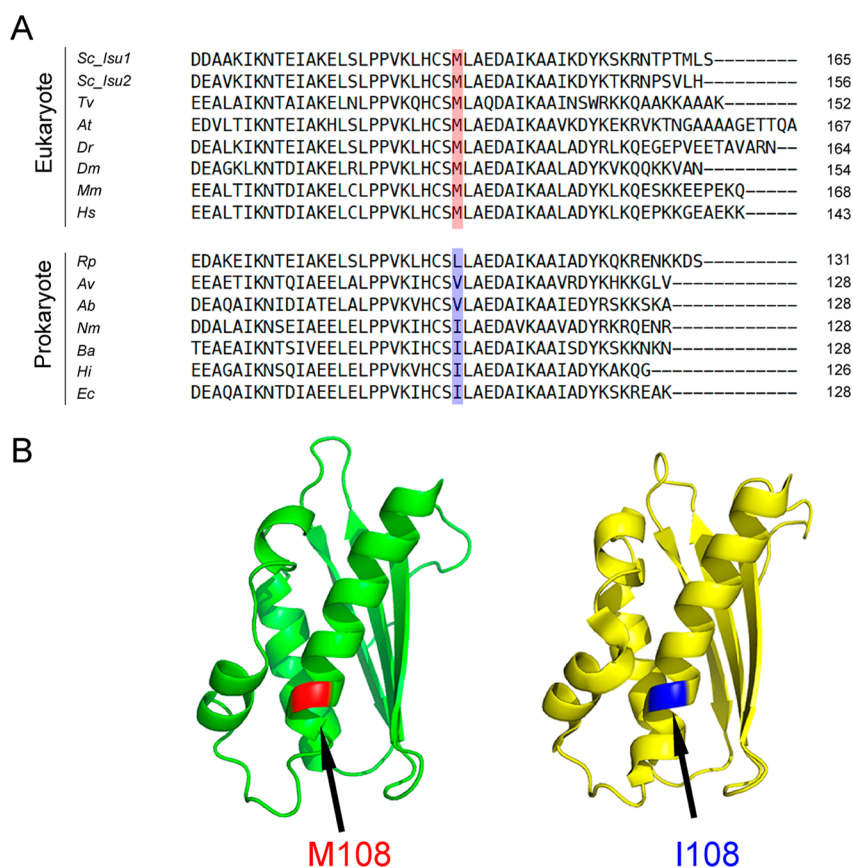


Figure 1. (A) Comparison of the sequence-aligned C-terminal regions of eukaryotic and prokaryotic scaffold proteins indicating the conservation of a methionine residue in eukaryotes (red) and an isoleucine residue in prokaryotes (blue). Abbreviations: Ab, *Acinetobacter baumannii*; At, *Arabidopsis thaliana*; Av, *Azotobacter vinelandii*; Ba, *Buchnera aphidicola*; Dm, *Drosophila melanogaster*; Dr, *Danio rerio*; Ec, *Escherichia coli*; Hi, *Haemophilus influenzae*; Hs, *Homo sapiens*; Mm, *Mus musculus*; Nm, *Neisseria meningitidis*; Rp, *Rickettsia prowazekii*; Sc, *Saccharomyces cerevisiae*; Tv, *Trichomonas vaginalis*. (B) NMR structures of the structured states of the (green) mouse ISCU (PDB entry 1WFZ) and (yellow) *H. influenzae* IscU (PDB entry 1R9P)³⁴ with the position of the differentially conserved residue highlighted.

reactions.^{24,25} FXN has also been shown to enhance sulfur transfer and control entry of iron into ISCU.^{26–28} However, the discovery in yeast of an Isu1 mutant that obviates the requirement for frataxin has presented a strong argument against frataxin being the primary iron donor.^{29–31} In this mutant of the scaffold protein, a methionine, which is invariant in mitochondrial ISCU proteins, is substituted with isoleucine, which is the homologous residue in bacterial IscU proteins (Figure 1). It has been shown that changing the Met residue to Ile in *Saccharomyces cerevisiae* Isu1 converts the yeast into a frataxin-independent organism and that changing Ile to Met in *E. coli* IscU turns the bacterium into a frataxin-dependent organism.^{32,33} The molecular mechanisms behind these effects have remained elusive.

In human mitochondria, assembly of a [2Fe-2S] cluster on scaffold protein ISCU involves reduced ferredoxin (rdFDX1 or rdFDX2),^{35–38} which donates electrons for the reduction of S⁰ generated by cysteine desulfurase. It has been shown in a yeast system (*S. cerevisiae*) that ferredoxin (Yah1), scaffold protein (Isu1), and frataxin (Yfh1) bind simultaneously to the cysteine desulfurase to form a large complex.³⁵ By contrast, in the *E. coli* system, the binding of bacterial frataxin (CyaY) and ferredoxin (Fdx) to the IscS–IscU complex was found to be mutually exclusive.^{39,40} CyaY has been shown to be a negative regulator of Fe–S cluster assembly in *E. coli*.⁴¹

Wild-type human ISCU, like its *E. coli* homologue IscU,^{42,43} has been found to populate two interconverting conformational states: one structured (S) and one dynamically disordered (D). Here, we demonstrate that both ISCU(M108I) and another variant, ISCU(D39V), are fully structured. We have compared the *in vitro* functional properties of wild-type ISCU and these two structured variants in the cysteine desulfurase reaction and in overall Fe–S cluster assembly. Additional NMR titration studies revealed that rdFDX2 displaces FXN from the (NIA)₂ complex when the bound scaffold protein is ISCU(M108I) but not when it is wild-type ISCU. These results shed new light on the mechanism of the observed frataxin bypassing activity of ISCU(M108I).

MATERIALS AND METHODS

Protein Expression and Purification. Unlabeled and uniformly ¹⁵N-labeled samples of ISCU, unlabeled (NIA)₂, unlabeled and [U-¹⁵N]FXN^{81–210}, and unlabeled FDX2 were produced and purified as described previously.^{19,38,43} The expression plasmids for ISCU variants M108I and D39V were produced by using the Polymerase Incomplete Primer Extension (PIPE) site-directed mutagenesis method.⁴⁴ Unlabeled, uniformly ¹⁵N-labeled, and uniformly ¹⁵N- and ¹³C-labeled samples of ISCU(M108I) and ISCU(D39V) were produced and purified as described previously for ISCU.⁴³

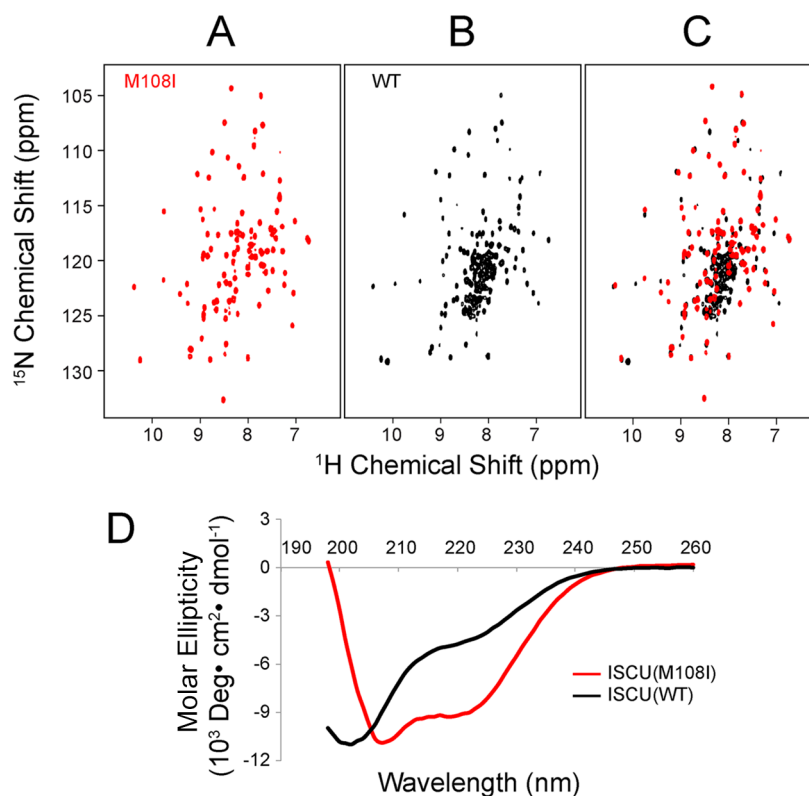


Figure 2. Structural differences between ISCU and ISCU(M108I). (A) 2D ^1H - ^{15}N TROSY-HSQC spectrum of $[\text{U}-^{15}\text{N}]$ ISCU(M108I). (B) 2D ^1H - ^{15}N TROSY-HSQC spectrum of $[\text{U}-^{15}\text{N}]$ ISCU. (C) Overlay of spectra from panels A and B. (D) CD spectra of ISCU(M108I) (red) and ISCU (black).

NMR Spectroscopy. NMR spectra were collected at the National Magnetic Resonance Facility at Madison on a 600 or 750 MHz (^1H) Bruker NMR spectrometer equipped with z-gradient cryogenic probes. The buffer used for NMR samples (HNT buffer) contained 20 mM HEPES (pH 7.6), 150 mM NaCl, 2 mM TCEP, and 7% D_2O as an NMR lock signal. All sample temperatures were regulated at 25 $^\circ\text{C}$. NMRPipe software was used to process the raw NMR data,⁴⁵ and NMRFAM-SPARKY⁴⁶ software was used to visualize and analyze the processed NMR data. All NMR experiments were performed once except for the NMR titration experiments, which were performed twice.

The backbone signals of $[\text{U}-^{13}\text{C},\text{U}-^{15}\text{N}]$ ISCU(D39V) and $[\text{U}-^{13}\text{C},\text{U}-^{15}\text{N}]$ ISCU(M108I) were assigned by collecting and analyzing the following NMR spectra: two-dimensional (2D) ^1H - ^{15}N HSQC, three-dimensional (3D) HNCA, 3D HNCO, 3D HNCACB, and 3D CBCA(CO)NH. All 3D spectra were recorded using non-uniform sampling (NUS) with a sampling rate of 36% and were processed using NESTA⁴⁷ and NMRPipe. The PINE server⁴⁸ was used for the automatic assignment of the backbone signals followed by manual refinements. The assignments of the backbone signals of ISCU(M108I) and ISCU(D39V) have been deposited in the BMRB⁴⁹ as entries 27088 and 27089, respectively.

To study the interaction between ISCU(M108I) and $(\text{NIA})_2$, a 0.3 mM sample of $[\text{U}-^{15}\text{N}]$ ISCU(M108I) was placed in a 5 mm Shigemi NMR tube, and 2D ^1H - ^{15}N TROSY-HSQC spectra were collected before and after titration with unlabeled $(\text{NIA})_2$.

Chemical shift perturbations ($\Delta\delta_{\text{HN}}$ absolute value in parts per million) were calculated with eq 1:

$$\Delta\delta_{\text{HN}} = [(\Delta\delta_{\text{H}})^2 + (\Delta\delta_{\text{N}}/6)^2]^{1/2} \quad (1)$$

where $\Delta\delta_{\text{H}}$ and $\Delta\delta_{\text{N}}$ are the chemical shift changes in the ^1H and ^{15}N dimensions, respectively.

Circular Dichroism (CD) Spectroscopy. The sample buffer used in circular dichroism (CD) experiments contained 20 mM NaH_2PO_4 and 50 mM NaCl (pH 8). The solutions were placed in 1 mm path length quartz cuvettes. The concentrations of ISCU and ISCU(M108I) were both 20 μM . Far-ultraviolet CD spectra of the samples were collected at 25 $^\circ\text{C}$ with an Aviv 202SF CD spectrophotometer.

Isothermal Titration Calorimetry (ITC) Measurement.

A Nano ITC (TA Instruments) system was used to investigate the interactions between ISCU(M108I) and $(\text{NIA})_2$. Both $(\text{NIA})_2$ and ISCU(M108I) were dialyzed extensively against HNT buffer. The sample cell (169 μL) contained 0.1 mM ISCU(M108I), and the syringe (50 μL) contained 1.1 mM $(\text{NIA})_2$. Twenty aliquots of 2.5 μL of $(\text{NIA})_2$ were injected into the sample cell, and the heat generated after each injection was measured. NanoAnalyse software was used in processing and fitting the ITC data.

Cysteine Desulfurase Assay and *in Vitro* Fe-S Cluster Assembly Reaction.

The protein samples used in the cysteine desulfurase assay (three replicates) and Fe-S cluster assembly experiments (two replicates) were prepared in an anaerobic chamber (Coy Laboratory) with samples buffer-exchanged extensively prior to data collection with anaerobic buffer containing 20 mM HEPES (pH 7.6) and 150 mM NaCl (HN buffer). The reaction volumes in all the experiments were kept at 1 mL. A Shimadzu UV-1700 UV/vis spectrophotometer with a temperature control unit was used to collect the spectra, and

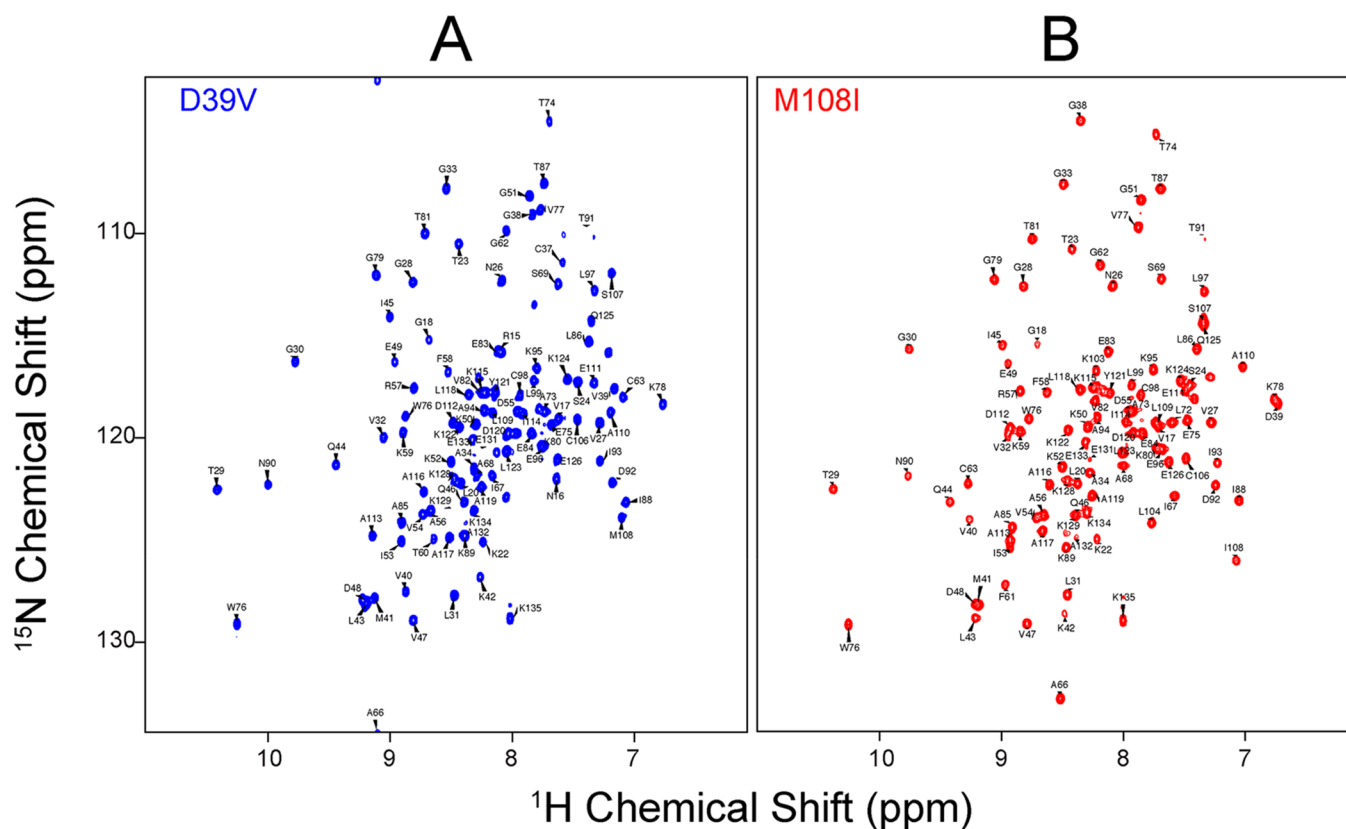


Figure 3. ^1H – ^{15}N TROSY-HSQC spectra annotated with assignments of backbone ^1H – ^{15}N signals of (A) ISCU(D39V) and (B) ISCU(M108I).

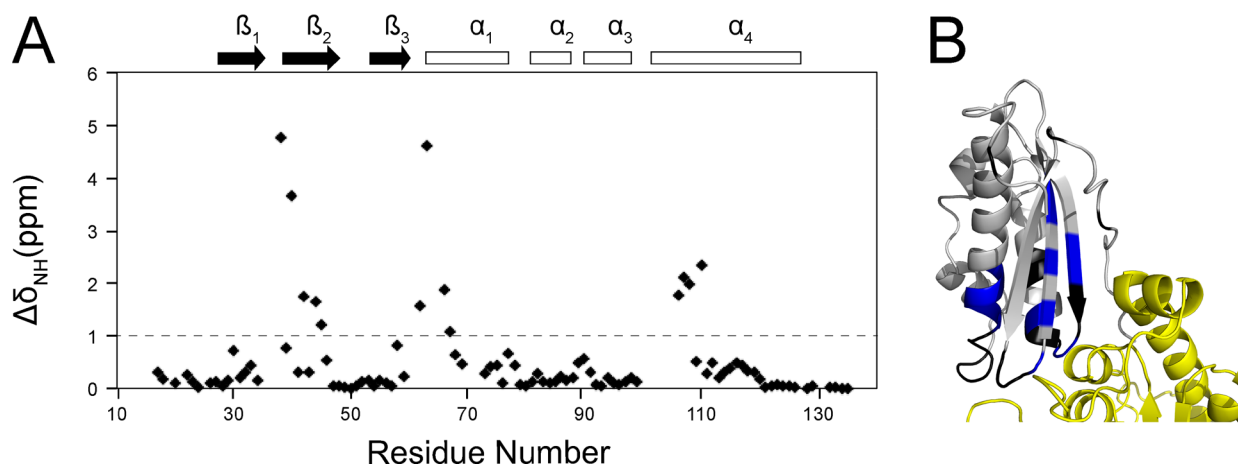


Figure 4. (A) Chemical shift differences between the ^1H – ^{15}N peaks of ISCU(D39V) and ISCU(M108I). (B) Chemical shift differences of the two ISCU variants mapped onto the structure of the NFS1–ISCU subcomplex (PDB entry SWLW). Color code: gray, no significant differences; blue, large chemical shift differences ($\Delta\delta_{\text{NH}} > 1$ ppm); black, no assignment.

UVProbe 2.21 software (Shimadzu) was used in collecting and analyzing the data.

The cysteine desulfurase assay reaction mixtures (300 μL in HN buffer) contained 1 μM (NIA)₂. The reductant was 100 μM DTT; 50 μM *L*-cysteine was added to initiate the reaction. One or more of the following components were added to assess their effects on sulfide production: 10 μM ISCU, 10 μM FXN, and 10 μM ISCU(M108I). After anaerobic incubation at room temperature for 20 min, the reaction mixture was diluted to 800 μL , and 100 μL of 20 mM *N,N*-dimethyl-*p*-phenylenediamine in 7.2 M HCl and 100 μL of 30 mM FeCl₃ in 1.2 M HCl were added to quench the reaction and convert sulfide to methylene

blue. The quenched reaction mixture was incubated for 15 min at room temperature, and then the absorbance at 670 nm was measured and used to estimate the amount of sulfide by comparison to a standard curve obtained from known concentrations of Na₂S.

The *in vitro* Fe–S cluster reconstitution assays were performed as follows. Reaction mixtures (1 mL) prepared in the anaerobic chamber contained 100 μM DTT or rFDX2 as the reductant, 0.5 μM (NIA)₂, 25 μM ISCU, ISCU(M108I), or ISCU(D39V), and 100 μM (NH₄)₂Fe(SO₄)₂; 25 μM FXN was added in reactions with FXN. *L*-Cysteine (final concentration of 100 μM) was added to initiate each experiment. Samples were

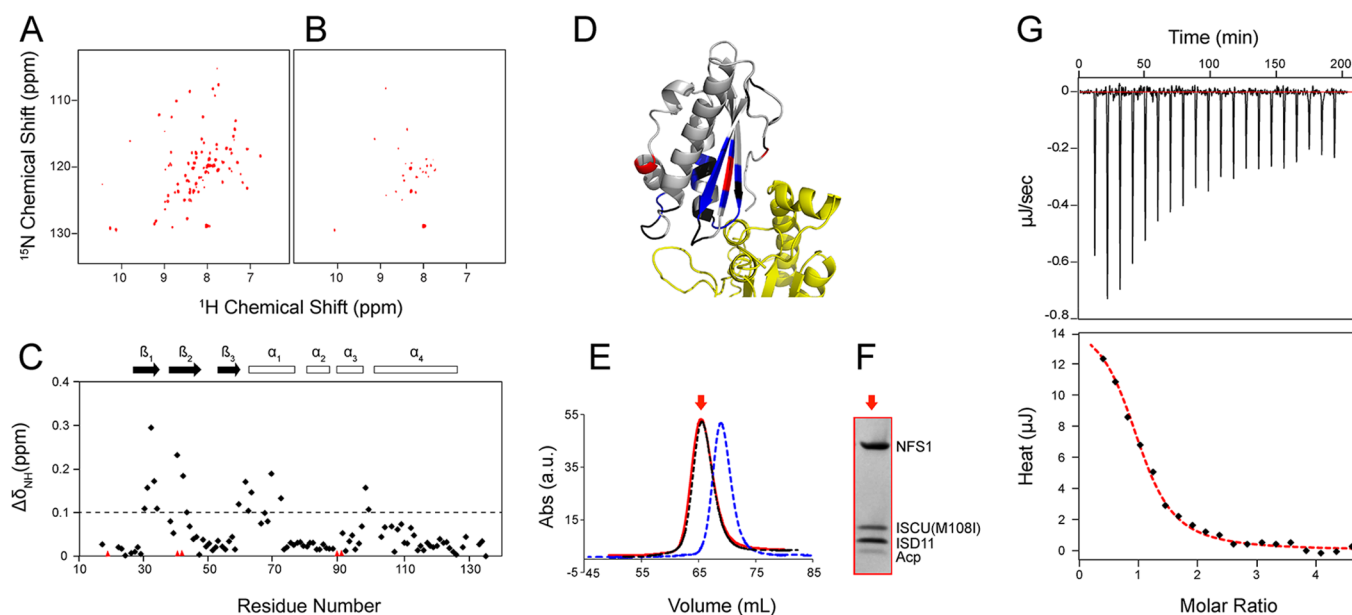


Figure 5. Investigation of the interaction between ISCU(M108I) and (NIA)₂. 2D ¹H–¹⁵N TROSY-HSQC spectra of [U-¹⁵N]ISCU(M108I) after the addition of (A) 0.5 and (B) 1.0 subunit equivalent of (NIA)₂. (C) CS perturbation ($\Delta\delta_{\text{NH}}$) of the ¹H–¹⁵N signals of [U-¹⁵N]ISCU(M108I) resulting from its interaction with (NIA)₂. The red triangles denote ¹H–¹⁵N peaks that are broadened beyond recognition. (D) CS perturbation from panel C mapped onto a portion of the structure of the NFS1–ISCU complex (PDB entry SWLW). Color code: gray, not significantly affected ($\Delta\delta_{\text{NH}} < 0.1$ ppm); blue, significant chemical shift changes ($\Delta\delta_{\text{NH}} > 0.1$ ppm); red, severe line broadening; black, no assignments. (E) Size-exclusion chromatography (SEC) profiles of (NIAU(M108I))₂ (red solid trace), (NIAU)₂ (black dashed trace), and (NIA)₂ (blue dashed trace). (F) SDS–PAGE analysis the SEC fraction (indicated by a red arrow pointing to the red trace in panel E) of (NIAU(M108I))₂ (note that the Acp band is weak because it stains weakly). (G) ITC analysis of the interactions between (NIA)₂ and ISCU(M108I). The top panels show peaks indicating heat released after each injection; the bottom panels show data points fitted to a single 1:1 binding constant to yield thermodynamic parameters.

then transferred to 1 cm path length quartz cuvettes, which were sealed with rubber septa, and ultraviolet–visible spectra were collected at 25 °C. The concentration of [2Fe-2S] was determined by use of a molar absorption coefficient (ϵ_{456}) of $9.2 \text{ mM}^{-1} \text{ cm}^{-1}$ per [2Fe-2S]²⁺ cluster.⁵⁰

RESULTS

The FXN-Bypassing Mutation of ISCU Shifts the S ⇌ D Equilibrium to the S State. We collected 2D ¹H–¹⁵N TROSY-HSQC spectra of the [U-¹⁵N]ISCU(M108I) and [U-¹⁵N]ISCU samples. Whereas the spectrum of ISCU(M108I) (Figure 2A) was consistent with a single structured state, the spectrum of [U-¹⁵N]ISCU (Figure 2B) showed evidence of two conformational states with ~30% of the molecules in the structured S state and 70% in the disordered D state as reported previously.⁴³ The peaks from ISCU(M108I) were found to overlap closely with the S-state peaks from ISCU (Figure 2C), indicating that their structures are similar. CD spectra (Figure 2D) also demonstrate that ISCU(M108) adopts a structured conformation while ISCU is partially disordered.

Assignment of the NMR Spectra of ISCU(M108I) and ISCU(D39V). Because ISCU(M108I) was found to be fully structured, we decided to compare its properties with those of another ISCU variant, ISCU(D39V), known to be structured.⁴³ By collecting and analyzing a series of 2D and 3D NMR spectra of protein samples labeled uniformly with ¹³C and ¹⁵N (see Materials and Methods), we assigned backbone ¹H^N–¹⁵N^H NMR signals from approximately 90% of the residues in both ISCU(M108I) and ISCU(D39V) (Figure 3). Signals from the remaining non-prolyl residues, including those in the “⁹⁹LPPVK¹⁰³” loop of each protein, were not observed, likely

as a result of internal dynamics. The backbone ¹H^N–¹⁵N^H signals exhibiting the largest chemical shift differences between the two variants ($\Delta\delta_{\text{NH}} > 1$ ppm) corresponded to residues G38, V40, K42, Q44, I45, F58, K59, G62, C63, A66, I67, and C106–A110 (Figure 4A). Many of the residues exhibiting chemical shift differences in the two variants map to the ISCU–NFS1 interface in the structure of the complex²¹ (Figure 4B). The ⁵⁸FKTFGCGSAI⁶⁷ region includes a cysteine residue that ligates the cluster. As expected, most other perturbations map to residues near the sequence differences (residues 39 and 108).

Investigation of the Interaction between ISCU(M108I) and Cysteine Desulfurase (NIA)₂. We used NMR spectroscopy to study the interaction between ISCU(M108I) and the cysteine desulfurase complex (NIA)₂. Titration of 0.5 and 1 subunit equivalent of unlabeled (NIA)₂ into [U-¹⁵N]ISCU(M108I) resulted in progressive changes in the ¹H–¹⁵N TROSY-HSQC spectra of [U-¹⁵N]ISCU(M108I) (Figure 5A,B). The peaks that shifted or broadened the most correspond to residues G18, G30–A34, V40–L43, K59, F61–C63, S69, L72, N90, T91, and C98 (Figure 5C). The (NIA)₂ binding site on ISCU(M108I) revealed by chemical shift perturbations (Figure 5D) agrees well with the X-ray structure of (NIAU)₂.²¹ The interaction between ISCU(M108I) and (NIA)₂ was further confirmed by size-exclusion chromatography (SEC) and sodium dodecyl sulfate–polyacrylamide gel electrophoresis (SDS–PAGE) (Figure 5E,F). The SEC profile of (NIAU(M108I))₂ was similar to that of (NIAU)₂ (Figure 5E). ITC was used to quantify the interaction between ISCU(M108I) and (NIA)₂. Titration of (NIA)₂ with ISCU(M108I) resulted in an endothermic reaction that was fitted to a 1:1 binding model with a K_d of $2.6 \pm 0.6 \mu\text{M}$ (Figure

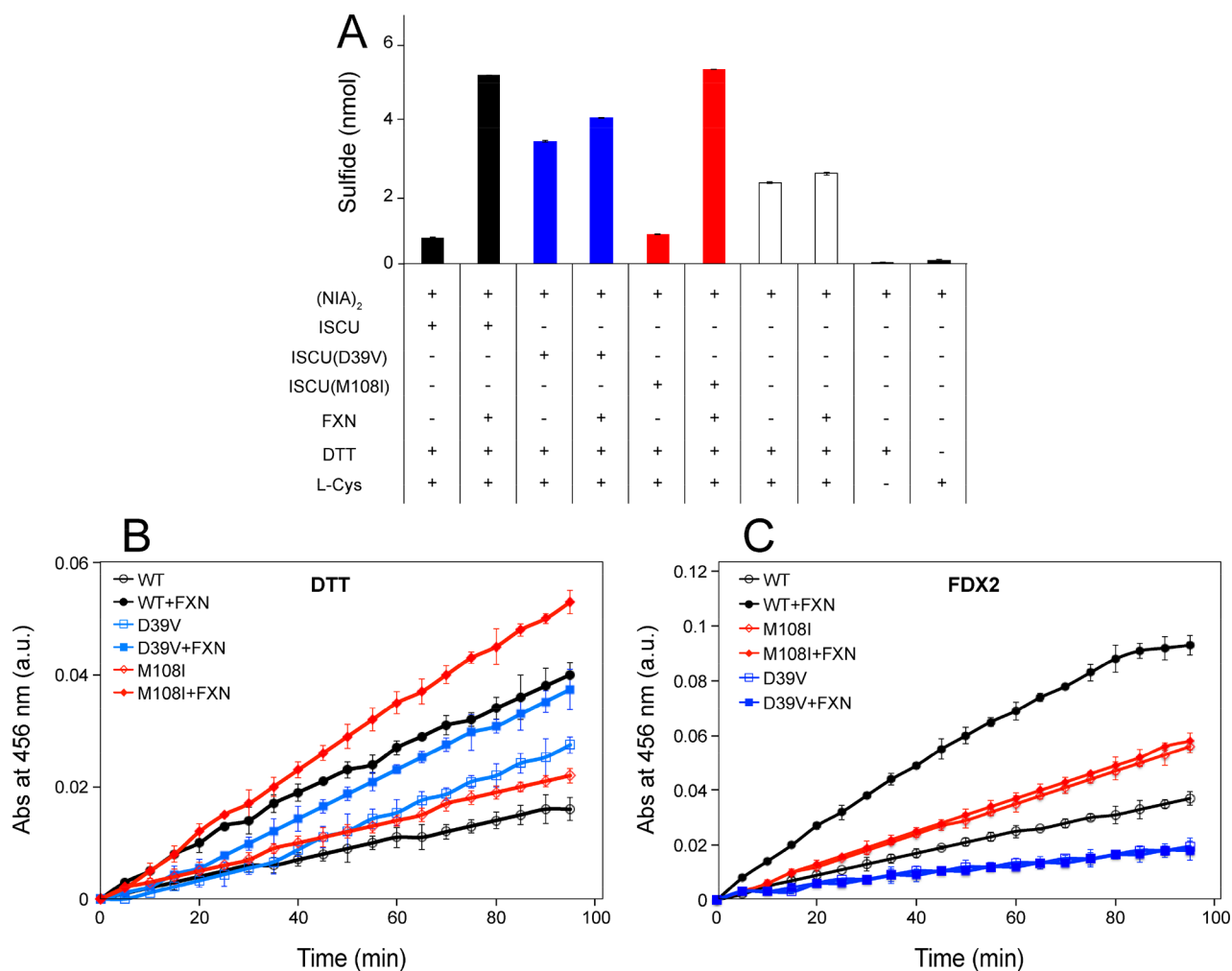


Figure 6. Evidence that the FXN bypassing phenotype of ISCU depends on the reducing agent. (A) Cysteine desulfurase activity assay of (NIA)₂. (B) Fe–S cluster reconstitution catalyzed by (NIA)₂ on ISCU, ISCU(M108I), and ISCU(D39V), with or without FXN, using DTT as the reducing agent. (C) Fe–S cluster reconstitution catalyzed by (NIA)₂ on ISCU, ISCU(M108I), and ISCU(D39V), with or without FXN, using rdFDX2 as the reducing agent. The conditions of each experiment are indicated in the figure.

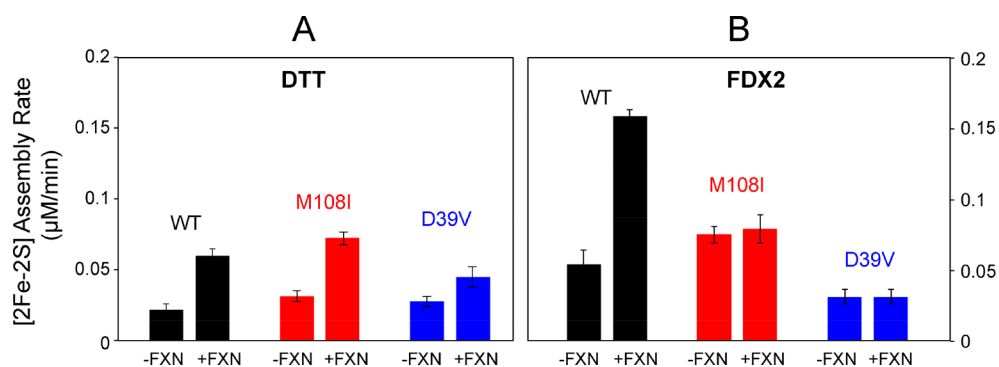


Figure 7. Quantification of Fe–S cluster assembly rates on ISCU variants with (A) DTT or (B) rFDX2 as the reducing agent.

5G). The binding constant is similar to that of (NIA)₂ and ISCU ($K_d = 1.7 \pm 0.4 \mu\text{M}$).⁵¹

Effects of Frataxin on Assembly of Clusters on the Different ISCU Variants. As a first step toward understanding the effects of ISCU mutations and the presence of FXN on the reactions involved in Fe–S cluster assembly, we investigated how they influence cysteine desulfurase activity with DTT as the reductant. No sulfide was produced by (NIA)₂ upon addition of L-cysteine or DTT alone (Figure 6A, rightmost two

bars). FXN alone had little effect on the cysteine desulfurase activity of (NIA)₂ when ISCU was not present (Figure 6A, white bars). ISCU alone had an inhibitory effect on the cysteine desulfurase activity (Figure 6A, by comparison of the first and seventh bars). Contrary to our expectation, FXN significantly enhanced the cysteine desulfurase activity of (NIA)₂ with both wild-type ISCU and ISCU(M108I) as the scaffold protein (Figure 6A, black and red bars). On the other hand, ISCU(D39V) showed strong desulfurase activity in the absence

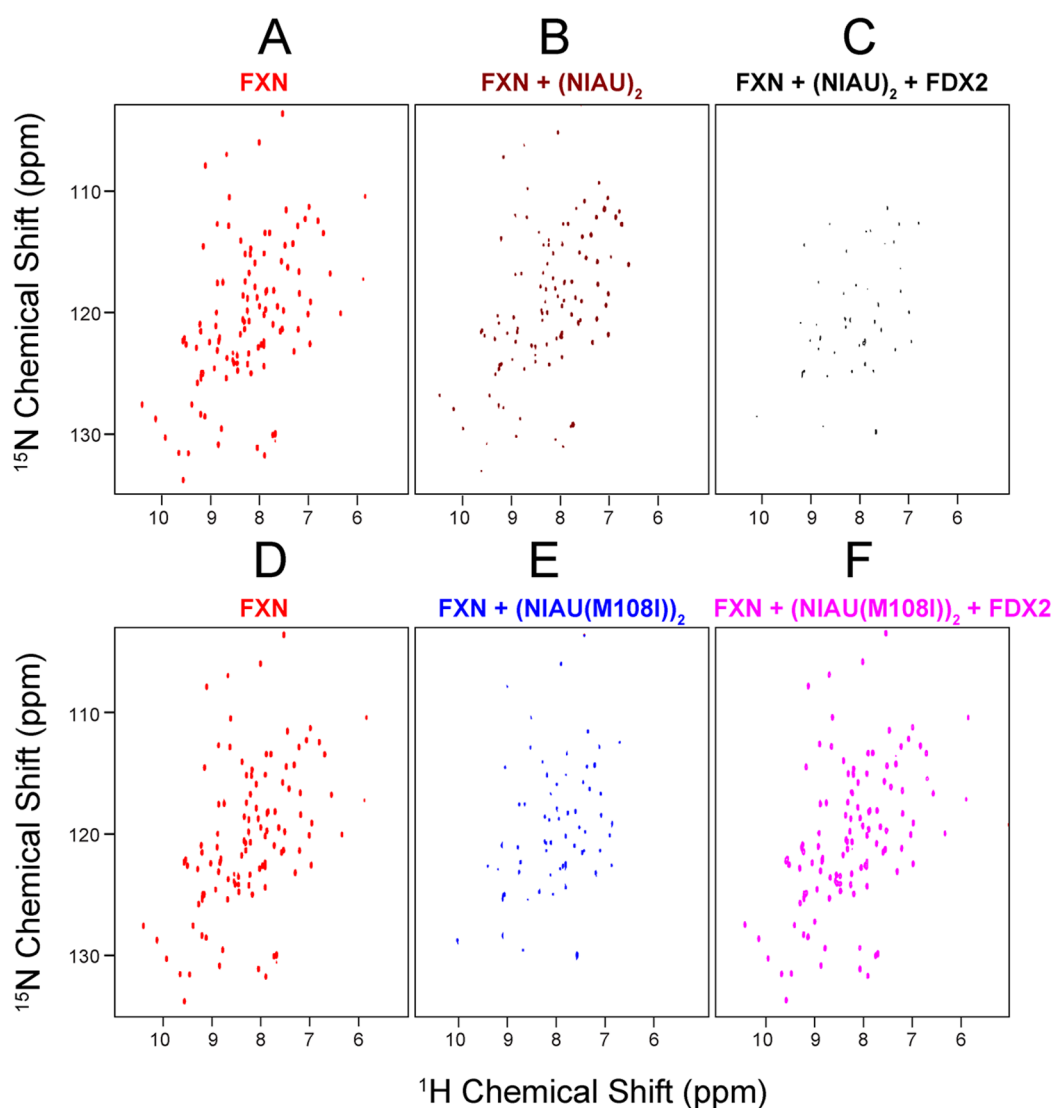


Figure 8. NMR spectra showing that FDX2 binds to (NIAU) $_2$ -FXN $_2$ without displacement of FXN but that FDX2 added to (NIAU(M108I)) $_2$ -FXN $_2$ displaces FXN. (A) ^1H - ^{15}N TROSY-HSQC spectrum of [U- ^{15}N]FXN. (B) ^1H - ^{15}N TROSY-HSQC spectrum of [U- ^{15}N]FXN after the addition of 0.5 subunit equivalent of unlabeled (NIAU) $_2$. (C) ^1H - ^{15}N TROSY-HSQC spectrum of [U- ^{15}N]FXN after the addition of 0.5 subunit equivalent of unlabeled (NIAU) $_2$ and 1.0 subunit equivalent of unlabeled FDX2. (D) ^1H - ^{15}N TROSY-HSQC spectrum of [U- ^{15}N]FXN. (E) ^1H - ^{15}N TROSY-HSQC spectrum of [U- ^{15}N]FXN after the addition of 0.5 subunit equivalent of unlabeled (NIAU(M108I)) $_2$. (F) ^1H - ^{15}N TROSY-HSQC spectrum of [U- ^{15}N]FXN after the addition of 0.5 subunit equivalent of unlabeled (NIAU(M108I)) $_2$ followed by the addition of 1.0 subunit equivalent of unlabeled FDX2.

of FXN, which increased only slightly with added FXN (Figure 6A, blue bars).

We next investigated the effect of FXN on *in vitro* Fe-S cluster assembly with DTT as the reductant (Figures 6B and 7A). Surprisingly, FXN showed an even stronger stimulating effect on Fe-S cluster assembly on ISCU(M108I) than on wild-type ISCU (Figure 6B, black and red, and Figure 7A). However, when we used rdFDX2, the likely physiologically relevant reductant in human mitochondrial Fe-S cluster biosynthesis,^{35,38} we obtained very different results. Although FXN stimulated the rate of *in vitro* Fe-S cluster assembly on wild-type ISCU, it had little effect on the rate of cluster assembly on either ISCU(M108I) or ISCU(D39V) (Figures 6C and 7B). The rate of cluster assembly on ISCU(M108I) (with or without FXN) was 50% higher than on wild-type ISCU in the absence of FXN. By contrast, the rate of cluster assembly on ISCU(D38V) (with or without FXN) was approximately half of

that of wild-type ISCU in the absence of FXN (Figures 6C and 7B).

Differential Effects of ISCU Variants on the NIAU-FXN-FDX2 Complex. We followed changes in the ^1H - ^{15}N TROSY-HSQC spectrum of [U- ^{15}N]FXN upon the addition of 0.5 subunit equivalent of (NIAU) $_2$ or (NIAU(M108I)) $_2$ complexes purified by SEC. In each case, the FXN peaks exhibited severe line broadening indicative of FXN binding to these complexes (panels A and B and panels D and E of Figure 8). Next, we added 1.0 subunit equivalent of unlabeled FDX2 to each of the solutions. In the case of (NIAU) $_2$, the addition of FDX2 led to further line broadening, which is consistent with partial formation of a larger (NIAU) $_2$ -FXN $_2$ -FDX $_2$ complex (Figure 8C). In the case of (NIAU(M108I)) $_2$, however, the addition of FDX2 led to peak sharpening and the reemergence of missing peaks, which is consistent with displacement of [U- ^{15}N]FXN from the (NIAU(M108I)) $_2$ complex by FDX2

(Figure 8F). In a similar experiment, FDX2 was found to displace $[U-^{15}N]FXN$ from the $(NIAU(D39V))_2$ complex (data not shown).

DISCUSSION

ISCU(M108I) was termed the “FXN bypassing mutant”,²⁹ because it appeared to allow functioning of iron–sulfur protein biosynthesis in the absence of frataxin in yeast. We found that ISCU(M108I) is fully structured (Figure 2). Incidentally, the authors of the recent X-ray structure of $(NIAU)_2$ ²¹ chose to use the M108I variant of ISCU “in the expectation that frataxin would be dispensable as part of the core ISC complex”. The fact that ISCU(M108I) is fully structured may have contributed to successful crystallization of the complex.

The D39V and D39A variants of *E. coli* IscU are fully structured.⁵² *In vivo* studies of IscU(D39A) in *Azotobacter vinelandii* showed that this variant forms a nondissociating, noncovalent complex with the cysteine desulfurase.⁵³ The homologous substitution in *S. cerevisiae* Isu(D37A) was found to worsen the defective growth phenotype caused by deletion of the frataxin homologue ($\Delta yfh1$).²⁹ We decided to include ISCU(D39V) in this study as a second example of a fully structured ISCU. Although both ISCU(M108I) and ISCU(D39V) are structured, we found significant differences in their structures as indicated by large chemical shift differences (Figure 4); these differences likely account for their different results in the cysteine desulfurase and cluster assembly reactions (Figure 7).

We compared the functional effects of FXN on $(NIA)_2$ complexes containing ISCU, ISCU(M108I), and ISCU(D39V) by performing two *in vitro* biochemical reactions: a cysteine desulfurase assay and a cluster assembly assay. The cysteine desulfurase assay is a nonphysiological reaction that is decoupled from cluster assembly and uses the chemical reductant DTT. In this assay, the rate of sulfide production was invariably higher in the presence of FXN than in its absence. The frataxin homologue in yeast (*Yfh1*) was shown to stimulate binding of cysteine to Nfs1 in the cysteine desulfurase reaction by exposing substrate binding sites, and it was proposed that Isu1(M108I) mimics this effect of *Yfh1*.³¹

By contrast, the cluster assembly assay utilizes Fe^{2+} as the iron source, and sulfur production is coupled to Fe–S cluster assembly. We compared the effects of two reductants on the Fe–S cluster assembly assay: DTT and reduced ferredoxin (rdFDX2). With nonphysiological DTT as the reductant (Figure 6B), FXN was observed to accelerate the Fe–S cluster assembly reaction with all three ISCU variants, with the relative enhancements decreasing in the following order: ISCU(M108I) > ISCU > ISCU(D39V). With rdFDX2 (Figure 6C), in the absence of FXN, the relative Fe–S cluster assembly rates decreased in the following order: ISCU(M108I) > ISCU > ISCU(D39V). However, when FXN was present, the rate of Fe–S cluster assembly on ISCU increased greatly, but the reactions with ISCU(M108I) and ISCU(D39V) remained unchanged.

Our finding that, in the absence of FXN but in the presence of rdFDX2, the rate of cluster assembly on ISCU(M108I) is significantly higher than on ISCU is in line with earlier studies in yeast.²⁹ This higher rate of cluster assembly may explain, in part, why the ISCU(M108I) variant in yeast cells has been found to escape the requirement for FXN.

Our results suggest that the dynamic interaction of proteins on the surface of cysteine desulfurase is key to understanding

the steps leading to Fe–S cluster formation on ISCU. We propose that the mechanism for the failure of FXN to stimulate Fe–S cluster assembly on ISCU(M108I) or ISCU(D39V) is the displacement of FXN by ferredoxin (FDX2). Our NMR studies showed that, whereas with ISCU, FDX2 binds to $(NIAUF)_2$ to form a larger complex, with the mutant ISCU(M108I), the addition of FDX2 displaces FXN (Figure 8). The displacement of FXN by FDX2 from the $(NIAU(M108I)F)_2$ complex is analogous to what was seen in the *E. coli* system, where the binding of bacterial frataxin and the binding of ferredoxin to the IscS–IscU complex were found to be mutually exclusive.^{39,40} However, the binding of FDX2 to $(NIAUF)_2$ is analogous to that in the yeast system in which the ferredoxin (*Yah1*) was shown to bind (*Nfs1*–*Isd11*–*Isu1*–*Yfh1*) and form a larger complex.³⁵ Both results can be explained by overlapping binding sites for frataxin and ferredoxin, but it appears that the relative binding affinities of frataxin and ferredoxin for the different cysteine desulfurases determine the consequences. With $(NIAU(M108I))_2$, FDX2 binds more tightly and FXN is displaced, leading to loss of frataxin stimulation, whereas with IscS–IscU, *CyaY* binds more tightly and Fdx is displaced, leading to inhibition by *CyaY*.³⁹ The complementary mutation (I108M) in *E. coli* IscU was found to render the cells dependent on *CyaY* for viability.³³ In this case, we hypothesize that IscU(I108M) may prevent IscX binding and, instead, enables the simultaneous binding of IscU(I108M), *CyaY*, and reduced ferredoxin to IscS.

More studies are needed to pin down the mechanism behind the stimulatory effect of FXN over free Fe^{2+} in solution. In the cysteine desulfurase reaction, the binding of FXN may serve to open the binding site of the dimeric NFS1 to better allow entry of reactants (*L*-cysteine and DTT) and the exit of products (sulfide and *L*-alanine). In the more physiological cluster assembly reaction, FXN in binding to NFS1 may position its bound iron for optimal transfer to ISCU. The number of iron ions transferred in each step has not been determined definitively, although a secondary iron binding site on Isu1 from *S. cerevisiae* has been suggested.⁵⁴ The concentration of free Fe^{2+} in the mitochondrial matrix is exceedingly low.⁵⁵ Thus, some other bound form of Fe^{2+} must be the source of the iron that recharges FXN.

AUTHOR INFORMATION

Corresponding Author

*Department of Biochemistry, University of Wisconsin—Madison, 433 Babcock Dr., Madison, WI 53706. Telephone: 608-263-9349. E-mail: jmarkley@wisc.edu.

ORCID

John L. Markley: 0000-0003-1799-6134

Author Contributions

K.C. and J.L.M. designed research. K.C., R.O.F., and M.T. performed research. R.O.F., M.T., and K.C. contributed new reagents and analytical tools. K.C., M.T., and J.L.M. analyzed data. K.C. and J.L.M. wrote the paper.

Funding

Initial support was from National Institutes of Health Grant U01GM094622; current funding is from the Department of Biochemistry, University of Wisconsin—Madison.

Notes

The authors declare no competing financial interest.

ACKNOWLEDGMENTS

NMR spectra were collected at the National Magnetic Resonance Facility at Madison, which receives support from National Institutes of Health Grant P41GM103399.

ABBREVIATIONS

Acp, holo form of *E. coli* acyl carrier protein; ACP, holo form of mature human mitochondrial acyl carrier protein; Af, *Archaeoglobus fulgidus*; CyaY, frataxin (*E. coli*); DTT, dithiothreitol; FDX2, ferredoxin 2 (human mitochondrial); Fe–S, iron–sulfur; FXN, mature form of human frataxin (FXN^{81–210}); HSQC, heteronuclear single-quantum correlation; IscS, cysteine desulfurase (*E. coli*); IscU, scaffold protein for Fe–S cluster assembly (*E. coli*); ISCU, scaffold protein for Fe–S cluster assembly (human mitochondrial); ISD11 (also known as LYRM4), small protein that binds tightly to NFS1 and is required for its activity; ITC, isothermal titration calorimetry; NFS1, cysteine desulfurase (human mitochondrial); (NIA)₂, [NFS1]₂:[ISD11]₂:[Acp]₂; (NIAU)₂, [NFS1]₂:[ISD11]₂:[Acp]₂:[ISCU]₂; (NIAUF)₂, [NFS1]₂:[ISD11]₂:[Acp]₂:[ISCU]₂:[FXN]₂; NMR, nuclear magnetic resonance; PDB, Protein Data Bank; rfdFX, reduced ferredoxin; TROSY, transverse relaxation-optimized spectroscopy; U-¹⁵N, uniform labeling with the stable isotope nitrogen-15; Yah1, ferredoxin (yeast); Yfh1, frataxin (yeast).

REFERENCES

- (1) Beinert, H., Holm, R. H., and Munck, E. (1997) Iron-sulfur clusters: Nature's modular, multipurpose structures. *Science* 277 (5326), 653–659.
- (2) Fontecave, M. (2006) Iron-sulfur clusters: ever-expanding roles. *Nat. Chem. Biol.* 2 (4), 171–4.
- (3) Lill, R. (2009) Function and biogenesis of iron-sulphur proteins. *Nature* 460 (7257), 831–8.
- (4) Lill, R., and Muhlenhoff, U. (2005) Iron-sulfur-protein biogenesis in eukaryotes. *Trends Biochem. Sci.* 30 (3), 133–41.
- (5) Johnson, D. C., Dean, D. R., Smith, A. D., and Johnson, M. K. (2005) Structure, function, and formation of biological iron-sulfur clusters. *Annu. Rev. Biochem.* 74, 247–81.
- (6) Py, B., and Barras, F. (2010) Building Fe-S proteins: bacterial strategies. *Nat. Rev. Microbiol.* 8 (6), 436–46.
- (7) Maio, N., and Rouault, T. A. (2015) Iron-sulfur cluster biogenesis in mammalian cells: New insights into the molecular mechanisms of cluster delivery. *Biochim. Biophys. Acta, Mol. Cell Res.* 1853 (6), 1493–1512.
- (8) Rouault, T. A. (2015) Mammalian iron-sulphur proteins: novel insights into biogenesis and function. *Nat. Rev. Mol. Cell Biol.* 16 (1), 45–55.
- (9) Braymer, J. J., and Lill, R. (2017) Iron-sulfur cluster biogenesis and trafficking in mitochondria. *J. Biol. Chem.* 292 (31), 12754–12763.
- (10) Rouault, T. A. (2012) Biogenesis of iron-sulfur clusters in mammalian cells: new insights and relevance to human disease. *Dis. Models & Mech.* 5 (2), 155–64.
- (11) Stehling, O., Wilbrecht, C., and Lill, R. (2014) Mitochondrial iron-sulfur protein biogenesis and human disease. *Biochimie* 100, 61–77.
- (12) Kispal, G., Csere, P., Prohl, C., and Lill, R. (1999) The mitochondrial proteins Atm1p and Nfs1p are essential for biogenesis of cytosolic Fe/S proteins. *EMBO J.* 18 (14), 3981–3989.
- (13) Pandey, A., Golla, R., Yoon, H., Dancis, A., and Pain, D. (2012) Persulfide formation on mitochondrial cysteine desulfurase: enzyme activation by a eukaryote-specific interacting protein and Fe-S cluster synthesis. *Biochem. J.* 448 (2), 171–87.
- (14) Angerer, H. (2015) Eukaryotic LYR proteins interact with mitochondrial protein complexes. *Biology (Basel, Switz.)* 4 (1), 133–50.

(15) Angerer, H. (2013) The superfamily of mitochondrial Complex1 LYR motif-containing (LYRM) proteins. *Biochem. Soc. Trans.* 41 (5), 1335–41.

(16) Kastaniotis, A. J., Autio, K. J., Keratar, J. M., Monteuis, G., Makela, A. M., Nair, R. R., Pietikainen, L. P., Shvetsova, A., Chen, Z., and Hiltunen, J. K. (2017) Mitochondrial fatty acid synthesis, fatty acids and mitochondrial physiology. *Biochim. Biophys. Acta, Mol. Cell Biol. Lipids* 1862 (1), 39–48.

(17) Beld, J., Lee, D. J., and Burkart, M. D. (2015) Fatty acid biosynthesis revisited: structure elucidation and metabolic engineering. *Mol. Biosyst.* 11 (1), 38–59.

(18) Van Vranken, J. G., Jeong, M. Y., Wei, P., Chen, Y. C., Gygi, S. P., Winge, D. R., and Rutter, J. (2016) The mitochondrial acyl carrier protein (ACP) coordinates mitochondrial fatty acid synthesis with iron sulfur cluster biogenesis. *eLife* 5, e17828.

(19) Cai, K., Frederick, R. O., Tonelli, M., and Markley, J. L. (2017) Mitochondrial cysteine desulfurase and ISD11 coexpressed in *Escherichia coli* yield complex containing acyl carrier protein. *ACS Chem. Biol.* 12 (4), 918–921.

(20) Cory, S. A., Van Vranken, J. G., Brignole, E. J., Patra, S., Winge, D. R., Drennan, C. L., Rutter, J., and Barondeau, D. P. (2017) Structure of human Fe-S assembly subcomplex reveals unexpected cysteine desulfurase architecture and acyl-ACP-ISD11 interactions. *Proc. Natl. Acad. Sci. U. S. A.* 114 (27), E5325–E5334.

(21) Boniecki, M. T., Freibert, S. A., Muhlenhoff, U., Lill, R., and Cygler, M. (2017) Structure and functional dynamics of the mitochondrial Fe/S cluster synthesis complex. *Nat. Commun.* 8 (1), 1287.

(22) Kim, J. H., Bothe, J. R., Frederick, R. O., Holder, J. C., and Markley, J. L. (2014) Role of IscX in iron-sulfur cluster biogenesis in *Escherichia coli*. *J. Am. Chem. Soc.* 136 (22), 7933–7942.

(23) Vaubel, R. A., and Isaya, G. (2013) Iron-sulfur cluster synthesis, iron homeostasis and oxidative stress in Friedreich ataxia. *Mol. Cell. Neurosci.* 55, 50–61.

(24) Cook, J. D., Kondapalli, K. C., Rawat, S., Childs, W. C., Murugesan, Y., Dancis, A., and Stemmler, T. L. (2010) Molecular details of the yeast frataxin-Isu1 interaction during mitochondrial Fe-S cluster assembly. *Biochemistry* 49 (40), 8756–65.

(25) Yoon, T., and Cowan, J. A. (2003) Iron-sulfur cluster biosynthesis. Characterization of frataxin as an iron donor for assembly of [2Fe-2S] clusters in ISU-type proteins. *J. Am. Chem. Soc.* 125 (20), 6078–84.

(26) Parent, A., Elduque, X., Cornu, D., Belot, L., Le Caer, J. P., Grandas, A., Toledano, M. B., and D'Autreaux, B. (2015) Mammalian frataxin directly enhances sulfur transfer of NFS1 persulfide to both ISCU and free thiols. *Nat. Commun.* 6, 5686.

(27) Bridwell-Rabb, J., Fox, N. G., Tsai, C. L., Winn, A. M., and Barondeau, D. P. (2014) Human frataxin activates Fe-S cluster biosynthesis by facilitating sulfur transfer chemistry. *Biochemistry* 53 (30), 4904–13.

(28) Colin, F., Martelli, A., Clemancey, M., Latour, J. M., Gambarelli, S., Zeppieri, L., Birck, C., Page, A., Puccio, H., and Ollagnier de Choudens, S. (2013) Mammalian frataxin controls sulfur production and iron entry during de novo Fe4S4 cluster assembly. *J. Am. Chem. Soc.* 135 (2), 733–40.

(29) Yoon, H., Golla, R., Lesuisse, E., Pain, J., Donald, J. E., Lyver, E. R., Pain, D., and Dancis, A. (2012) Mutation in the Fe-S scaffold protein Isu bypasses frataxin deletion. *Biochem. J.* 441 (1), 473–80.

(30) Yoon, H., Knight, S. A., Pandey, A., Pain, J., Zhang, Y., Pain, D., and Dancis, A. (2014) Frataxin-bypassing Isu1: characterization of the bypass activity in cells and mitochondria. *Biochem. J.* 459 (1), 71–81.

(31) Pandey, A., Gordon, D. M., Pain, J., Stemmler, T. L., Dancis, A., and Pain, D. (2013) Frataxin directly stimulates mitochondrial cysteine desulfurase by exposing substrate-binding sites, and a mutant Fe-S cluster scaffold protein with frataxin-bypassing ability acts similarly. *J. Biol. Chem.* 288 (52), 36773–86.

(32) Yoon, H., Knight, S. A., Pandey, A., Pain, J., Turkarlan, S., Pain, D., and Dancis, A. (2015) Turning *Saccharomyces cerevisiae* into a frataxin-independent organism. *PLoS Genet.* 11 (5), e1005135.

- (33) Roche, B., Agrebi, R., Huguenot, A., Ollagnier de Choudens, S., Barras, F., and Py, B. (2015) Turning *Escherichia coli* into a frataxin-dependent organism. *PLoS Genet.* 11 (5), e1005134.
- (34) Ramelot, T. A., Cort, J. R., Goldsmith-Fischman, S., Kornhaber, G. J., Xiao, R., Shastry, R., Acton, T. B., Honig, B., Montelione, G. T., and Kennedy, M. A. (2004) Solution NMR structure of the iron-sulfur cluster assembly protein U (IscU) with zinc bound at the active site. *J. Mol. Biol.* 344 (2), 567–583.
- (35) Webert, H., Freibert, S. A., Gallo, A., Heidenreich, T., Linne, U., Amlacher, S., Hurt, E., Muhlenhoff, U., Banci, L., and Lill, R. (2014) Functional reconstitution of mitochondrial Fe/S cluster synthesis on Isu1 reveals the involvement of ferredoxin. *Nat. Commun.* 5, 5013.
- (36) Shi, Y., Ghosh, M., Kovtunovych, G., Crooks, D. R., and Rouault, T. A. (2012) Both human ferredoxins 1 and 2 and ferredoxin reductase are important for iron-sulfur cluster biogenesis. *Biochim. Biophys. Acta, Mol. Cell Res.* 1823 (2), 484–492.
- (37) Sheftel, A. D., Stehling, O., Pierik, A. J., Elsasser, H. P., Muhlenhoff, U., Webert, H., Hobler, A., Hannemann, F., Bernhardt, R., and Lill, R. (2010) Humans possess two mitochondrial ferredoxins, Fdx1 and Fdx2, with distinct roles in steroidogenesis, heme, and Fe/S cluster biosynthesis. *Proc. Natl. Acad. Sci. U. S. A.* 107 (26), 11775–80.
- (38) Cai, K., Tonelli, M., Frederick, R. O., and Markley, J. L. (2017) Human mitochondrial ferredoxin 1 (FDX1) and ferredoxin 2 (FDX2) both bind cysteine desulfurase and donate electrons for iron-sulfur cluster biosynthesis. *Biochemistry* 56 (3), 487–499.
- (39) Kim, J. H., Frederick, R. O., Reinen, N. M., Troupis, A. T., and Markley, J. L. (2013) [2Fe-2S]-Ferredoxin binds directly to cysteine desulfurase and supplies an electron for iron-sulfur cluster assembly but is displaced by the scaffold protein or bacterial frataxin. *J. Am. Chem. Soc.* 135 (22), 8117–20.
- (40) Yan, R., Konarev, P. V., Iannuzzi, C., Adinolfi, S., Roche, B., Kelly, G., Simon, L., Martin, S. R., Py, B., Barras, F., Svergun, D. I., and Pastore, A. (2013) Ferredoxin competes with bacterial frataxin in binding to the desulfurase IscS. *J. Biol. Chem.* 288 (34), 24777–87.
- (41) Adinolfi, S., Iannuzzi, C., Prischi, F., Pastore, C., Iametti, S., Martin, S. R., Bonomi, F., and Pastore, A. (2009) Bacterial frataxin CyaY is the gatekeeper of iron-sulfur cluster formation catalyzed by IscS. *Nat. Struct. Mol. Biol.* 16 (4), 390–6.
- (42) Kim, J. H., Füzéry, A. K., Tonelli, M., Ta, D. T., Westler, W. M., Vickery, L. E., and Markley, J. L. (2009) Structure and dynamics of the iron-sulfur cluster assembly scaffold protein IscU and its interaction with the cochaperone HscB. *Biochemistry* 48 (26), 6062–71.
- (43) Cai, K., Frederick, R. O., Kim, J. H., Reinen, N. M., Tonelli, M., and Markley, J. L. (2013) Human mitochondrial chaperone (mtHSP70) and cysteine desulfurase (NFS1) bind preferentially to the disordered conformation, whereas co-chaperone (HSC20) binds to the structured conformation of the iron-sulfur cluster scaffold protein (ISCU). *J. Biol. Chem.* 288 (40), 28755–70.
- (44) Klock, H. E., and Lesley, S. A. (2009) The Polymerase Incomplete Primer Extension (PIPE) method applied to high-throughput cloning and site-directed mutagenesis. *Methods Mol. Biol.* 498, 91–103.
- (45) Delaglio, F., Grzesiek, S., Vuister, G. W., Zhu, G., Pfeifer, J., and Bax, A. (1995) NMRPIPE - A multidimensional spectral processing system based on UNIX Pipes. *J. Biomol. NMR* 6 (3), 277–293.
- (46) Lee, W., Tonelli, M., and Markley, J. L. (2015) NMRFAM-SPARKY: enhanced software for biomolecular NMR spectroscopy. *Bioinformatics* 31 (8), 1325–7.
- (47) Sun, S., Gill, M., Li, Y., Huang, M., and Byrd, R. A. (2015) Efficient and generalized processing of multidimensional NUS NMR data: the NESTA algorithm and comparison of regularization terms. *J. Biomol. NMR* 62 (1), 105–17.
- (48) Lee, W., Westler, W. M., Bahrami, A., Eghbalnia, H. R., and Markley, J. L. (2009) PINE-SPARKY: graphical interface for evaluating automated probabilistic peak assignments in protein NMR spectroscopy. *Bioinformatics* 25 (16), 2085–2087.
- (49) Ulrich, E. L., Akutsu, H., Doreleijers, J. F., Harano, Y., Ioannidis, Y. E., Lin, J., Livny, M., Mading, S., Maziuk, D., Miller, Z., Nakatani, E., Schulte, C. F., Tolmie, D. E., Kent Wenger, R., Yao, H., and Markley, J. L. (2008) BioMagResBank. *Nucleic Acids Res.* 36 (Database), D402–D408.
- (50) Agar, J. N., Krebs, C., Frazzon, J., Huynh, B. H., Dean, D. R., and Johnson, M. K. (2000) IscU as a scaffold for iron-sulfur cluster biosynthesis: sequential assembly of [2Fe-2S] and [4Fe-4S] clusters in IscU. *Biochemistry* 39 (27), 7856–7862.
- (51) Cai, K., Tonelli, M., Frederick, R. O., and Markley, J. L. (2018) Interactions of iron-bound frataxin with ISCU and ferredoxin on the cysteine desulfurase complex leading to Fe-S cluster assembly. *J. Inorg. Biochem.*
- (52) Markley, J. L., Kim, J. H., Dai, Z., Bothe, J. R., Cai, K., Frederick, R. O., and Tonelli, M. (2013) Metamorphic protein IscU alternates conformations in the course of its role as the scaffold protein for iron-sulfur cluster biosynthesis and delivery. *FEBS Lett.* 587 (8), 1172–9.
- (53) Raulfs, E. C., O'Carroll, I. P., Dos Santos, P. C., Unciuleac, M. C., and Dean, D. R. (2008) *In vivo* iron-sulfur cluster formation. *Proc. Natl. Acad. Sci. U. S. A.* 105 (25), 8591–8596.
- (54) Rodrigues, A. V., Kandegedara, A., Rotondo, J. A., Dancis, A., and Stemmler, T. L. (2015) Iron loading site on the Fe-S cluster assembly scaffold protein is distinct from the active site. *BioMetals* 28 (3), 567–76.
- (55) Richardson, D. R., Lane, D. J., Becker, E. M., Huang, M. L., Whitnall, M., Suryo Rahmanto, Y., Sheftel, A. D., and Ponka, P. (2010) Mitochondrial iron trafficking and the integration of iron metabolism between the mitochondrion and cytosol. *Proc. Natl. Acad. Sci. U. S. A.* 107 (24), 10775–82.